Research Article

Yeole Shivraj Narayan*, Kode Jaya Prakash, Maddika Harinatha Reddy and B. Sridhar Babu*

Surface integrity studies in microhole drilling of Titanium Beta-C alloy using microEDM

https://doi.org/10.1515/jmbm-2024-0024
received July 11, 2024; accepted November 04, 2024

Abstract: Micro electro-discharge machining, commonly known as MicroEDM, is used in the manufacturing industry for micromachining due to its benefits over conventional manufacturing. Titanium and its alloys find their application in various sectors. Titanium Beta-C alloy is one such alloy, especially employed in the oilfield and underwater sectors. Various applications in these fields need to have microholes embedded in them. Moreover, these parts need to possess high strength and be corrosion-resistant. Hence, the surface integrity of this alloy is critical. The intent behind this investigation is to evaluate the surface integrity characteristics of Titanium Beta-C alloy by performing microhole drilling using microEDM process parameters. In this study, surface integrity characteristics like surface topography and morphology are investigated by drilling microholes using brass electrodes of 300 µm in L9 orthogonal array experiments. Pulse on time, pulse off time, voltage, and current as pulse parameters are employed. Responses measured are surface roughness (R_a), SEM microstructure, and energy dispersive X-ray analysis. This investigation shows the formation of irregular shapes of the craters on the surface of microholes drilled in Titanium Beta-C alloy. Additionally, these surfaces exhibit shallow crater depths and do not show the presence of cracks.

Keywords: microEDM, Titanium Beat-C alloy, surface roughness, EDXA

*** Corresponding author: Yeole Shivraj Narayan,** Department of Mechanical Engineering, Vallurupalli Nageswara Rao Vignana Jyothi Institute of Engineering and Technology, Hyderabad, India, e-mail: shivrajyeole@vnrvjiet.in
*** Corresponding author: B. Sridhar Babu,** Department of Mechanical Engineering, Malla Reddy Engineering College, Hyderabad, India, e-mail: bsridhar8477@mrec.ac.in
Kode Jaya Prakash: Department of Mechanical Engineering, Vallurupalli Nageswara Rao Vignana Jyothi Institute of Engineering and Technology, Hyderabad, India, e-mail: jayaprakash_k@vnrvjiet.in
Maddika Harinatha Reddy: Department of Mechanical Engineering, CVR College of Engineering, Hyderabad, India, e-mail: harinathareddy.maddika@cvr.ac.in

1 Introduction

Micro electro discharge machining (MicroEDM or µEDM) is a thermoerosion process that removes material from the workpiece *via* a series of discharge sparks. The fundamentals of the microEDM process are shown in Figure 1. The process entails two electrodes, a tool (anode) and a workpiece (cathode), connected in reverse polarity and separated by an interelectrode space in a dielectric bath. The use of deionized water as a dielectric serves insulation as well as cleaning of contaminants [1–3].

A charged electrode is brought near the workpiece in a bath of dielectric fluid. A sufficiently large electrical potential causes the fluid to break down into ionic (charged) fragments, allowing the electrical current to flow from the electrode to the workpiece. The electrical field is the strongest at a point where the distance between the electrode and the workpiece is the least. As the number of ionic (charged) particles increases, the insulating properties of the dielectric fluid begin to decrease along a narrow channel centered in the strongest part of the field. At this point, the voltage reaches its peak but with zero current. As the fluid becomes less of an insulator, a current is established. This is followed by a decrease in voltage. The increase in current builds up the heat, but the voltage keeps decreasing, leading to the vaporization of dielectric, electrode and work material. Consequently, a discharge strikes between the electrode and the workpiece. Expansion of newly forming and outwardly vapor bubbles is constrained by ionic flow toward the discharge channel. The ions are attracted by the newly formed strong electromagnetic field. The current persists to increase with dropping voltage. At the termination of on time, current and voltage stabilize. Some metal is ejected as maximum heat and pressure within the vapor bubble are reached. The pressure of the vapor bubble holds the layer of the molten metal beneath the discharge column. A superheated plasma comprises vaporized metals generated with intense current flowing through it. The generated heat during the plasma formation and expansion is transmitted to both electrodes *via* radiation heat transfer and ion and electron bombardment [4]. Material removal in

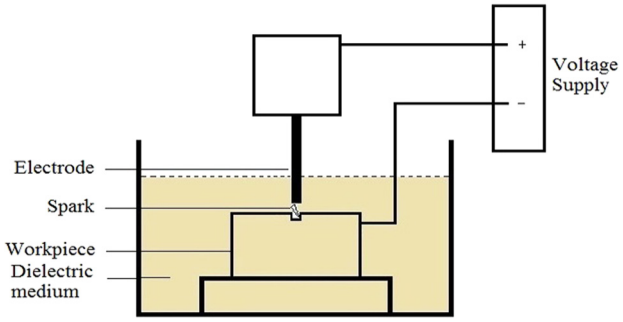

Figure 1: Principle of MicroEDM.

microEDM can be computed based on the average volume of material removed over machining time [5].

$$\text{Material removal rate} = \left\{\frac{\pi}{3}[r_{\text{Top}}^2 + r_{\text{Top}}r_{\text{Bottom}} + r_{\text{Bottom}}^2] \times h\right\} \div t. \quad (1)$$

Researchers have been exploring spark erosion mechanisms in the EDM process, resulting in the evolution of the microEDM process. These developments are steering EDM and its allied process, including microEDM as an apt process for diverse applications [6]. Drilling of microholes using EDM has also been attempted on steel (hardened) to attain a superior rate of material removal [7]. Microdrilling on shape memory alloys like Ni–Ti *via* brass and tungsten electrodes was performed to assess the influence of pulse parameters on the rate of material removal [8]. The rate of material removal was impacted by capacitance and voltage at the expense of surface quality. The increase in pulse time enhanced hardness but reduced the machining characteristics like the rate of material removal and the length of crack in EDM drilling on maraging steel alloy [9]. Material removal and roughness decreased with an increase in hardness. The reduction in the white layer thickness, the rate of tool wear, and heat affected zone was observed by employing high values of current and low pulse times [10]. Surface topographical features, inclusive of roughness and craters were researched in microEDM hole drilling by employing SEM. Roughness seemed to be affected by voltage, whereas the crater's shape was decided by variation in the voltage and current [11]. The effect of utilizing different electrode materials on the heat-affected zone was analyzed. The brass electrode provided a better finish, whereas copper gave a better rate of material removal. The effect of employing different dielectric fluids in the microEDM process was investigated. Demineralized water was found to be the best [12]. Taguchi and multiobjective-based optimization studies on different materials using EDM, microEDM, and varied forms have been performed to determine their impact on surface and machining characteristics *via* pulse parameters [13–18].

MicroEDM is an appealing process advancing abundant opportunities for furthering research. The majority of the studies have focused on pulse parameter optimization in microEDM. However, the nature of the process has been probed only on a few alloys. The spark erosion process typically produces a homogeneous surface texture, thereby indicating a need to have similar topography on roughness [19]. Titanium Beta-C alloy is an alloy employed in oilfields and underwater sectors, where the parts entail microholes. These parts need to possess high strength and be corrosion-resistant. Hence, the surface integrity of this alloy is critical. Accordingly, this investigation is aimed at drilling microholes on Titanium Beta-C alloy with a high deep hole aspect ratio using the microEDM process for understanding the surface integrity of microholes. The novelty of this study lies in its objective to achieve microholes with an aspect ratio of 16.67 on Titanium Beta-C alloy specimens using brass electrodes of 300 µm diameter, which could be beneficial in underwater applications.

2 Experimental details

Experimental investigations on micro-EDM aspects are limited to the optimization of surface finish and material removal rate. Hence, in this research, surface integrity studies, especially the surface roughness, surface morphology, and energy dispersive X-ray analysis (EDXA), are carried out on Titanium Beta-C alloy using a brass electrode on a microEDM machine. Titanium Beta-C alloy has distinct traits with reference to its durability and applications. First, Titanium Beta-C alloy possesses excellent corrosion resistance to liquids such as water and acids. It is expected to develop a shielding of oxide upon exposure to environments with higher oxygen concentrations. Second, it possesses a very high strength-to-weight ratio owing to its lower density and higher strength upon heat treatment.

Table 1: Constituents of Titanium Beta-C alloy

Element	C	Cr	Mo	V	Al	Fe	Fe	O	Zr	Ti
	0.05 max	5.5–6.5	3.5–4.5	7.5–8.5	3.0–4.0	0.3 max	0.3 max	0.03 max	3.5–4.5	Balance

Table 2: Physical properties of Titanium Beta-C alloy [20]

Property	Value
Density (g/cm^3)	4.81
Melting range (°C ± 15°C)	1649
Thermal conductivity (W/m K)	8.4
Mean coefficient of thermal expansion (0–100°C/°C)	9.4×10^{-6}
Mean coefficient of thermal expansion (0–300°C/°C)	9.7×10^{-6}
Beta Transus (°C ± 15°C)	793

Hence, microdrilled components of Titanium Beta-C alloy present potential candidature for oilfield and underwater applications. The composition and physical properties of Titanium Beta-C alloy are presented in Tables 1 and 2, respectively.

Taguchi's design of experiments is used to manage the experimental data. As per Taguchi's design of experiments, nine experiments are conducted on a microEDM machine using four input control factors at three different levels. Figure 2 depicts the microEDM machine employed for the experimentation, and Table 3 exhibits the specification of the microEDM machine.

However, to have more data available for analyzing the surface textural characteristics, three replicates of the 09 experiments are conducted resulting in a total of 27 microholes. The parameters and the experimental design employed are presented in Tables 4 and 5, respectively. Pulse parameter values are selected based on the machine specifications as well as trial experimentation.

3 Results and discussion

Figure 3(a) shows the dimensions of the specimens employed in the experimentation. Four specimens of Titanium Beta-C alloy with dimensions of 55 mm × 10 mm × 5 mm are used. A total of 27 microholes, as shown in Figure 3(b), are drilled on Titanium Beta-C alloy as per the experimental design shown in Table 5. Three replicates of 09 experiments are performed on the specimens, with the first replicate positioned in the middle of the first and second specimens, the second replicate at the edges of the specimens when clamped together, and the third replicate in the middle of the third and fourth specimens. 04 microholes each are drilled in the

Figure 2: Experimental setup on a Toolcraft V40506 microEDM machine.

Table 3: Machine specifications

Specification	Description
Make	Toolcraft
Model	V40506
Table (mm)	500 × 300
Worktank (mm)	800 × 500 × 350
X travel (mm)	325
Y travel (mm)	225
Z travel (mm)	200
Electrode	Brass
Hole size (μm)	100–500
Open circuit voltage (V)	100
Pulse time (μs)	1–9
Peak current (A)	1–25
Polarity	Reverse
Dielectric	Deionized water

Table 4: Pulse parameters in the experimentation

Factors/ levels	Pulse on time (A), μs	Pulse off time (B), μs	Voltage (C), V	Discharge current (D), A
1	1	3	30	3
2	5	6	60	4
3	9	9	90	5

Table 5: Experimentation design

Experiment no.	Factors and levels			
	A	B	C	D
1	1	1	1	1
2	1	2	2	2
3	1	3	3	3
4	2	1	2	3
5	2	2	3	1
6	2	3	1	2
7	3	1	3	2
8	3	2	1	3
9	3	3	2	1

middle of the first and third specimens, whereas 05 microholes each are drilled in the middle of the second and fourth specimens.

MicroEDM, akin to EDM, is a spark erosion process encompassing thermal shocks. Worn-out surfaces are characterized by considerable changes in physical and metallurgical features. These are due to the elevated spark temperature and the cooling effect of the dielectric. Surface integrity studies involve the study of surface topology and surface layer characteristics. Surface topographical studies include roughness, waviness, form errors, and flaws, whereas surface layer characterization includes morphology, residual stress, and hydrogen embrittlement phenomena [21]. Thermal cycles in the microEDM process alter notably. To comprehend the integrity of resulting surfaces, an investigation of microholes on Titanium Beta-C alloy is presented.

Table 6: Average surface roughness

Exp. no.	A	B	C	D	R_a (μm)
1	1	3	30	3	0.142
2	1	6	60	4	0.145
3	1	9	90	5	0.133
4	5	3	60	5	0.141
5	5	6	90	3	0.147
6	5	9	30	4	0.145
7	9	3	90	4	0.16
8	9	6	30	5	0.172
9	9	9	60	3	0.145

3.1 Surface roughness

Surface texture assessment involves roughness and waviness measurements. EDM and its allied microEDM process

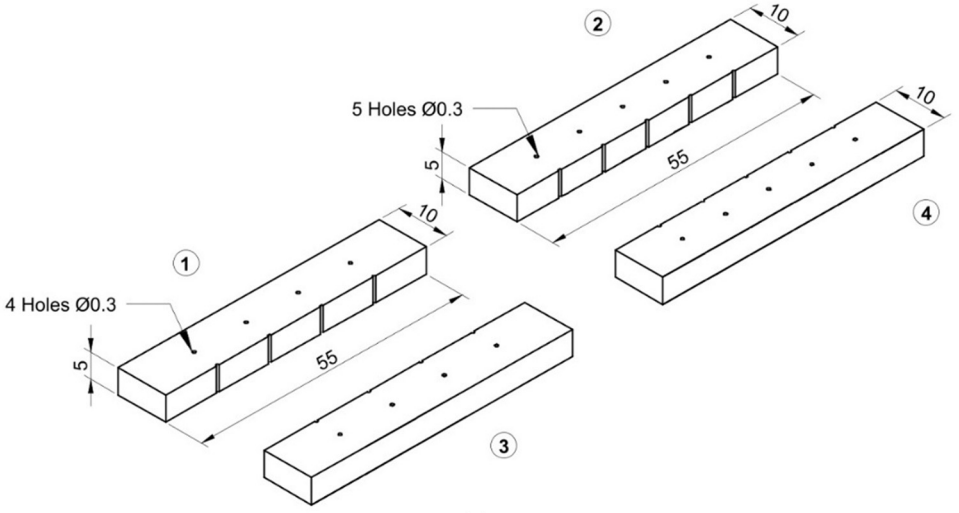

(a)

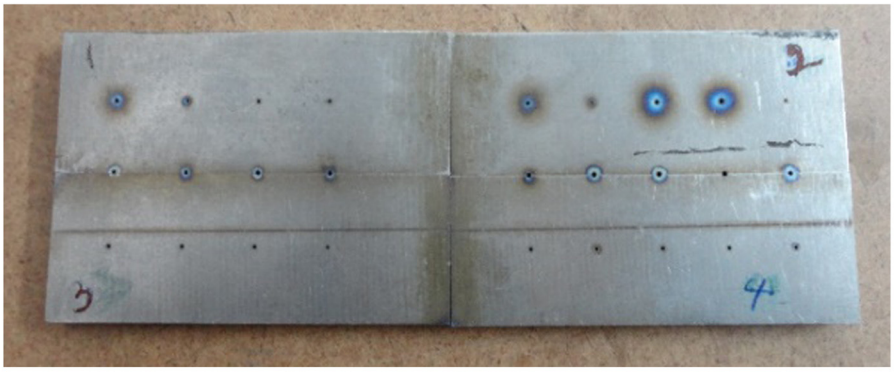

(b)

Figure 3: Microholes drilled on Titanium Beta-C alloy. (a) Specimen dimensions for microdrilling 27 microholes. (b) MicroEDM drilled 27 microholes.

Work Material	Effect of pulse parameters on surface roughness (µm) [Y-Axis]	
Titanium Beta-C alloy	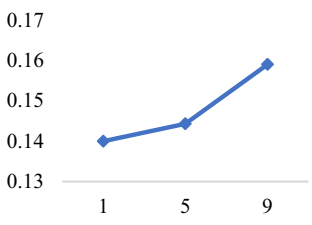	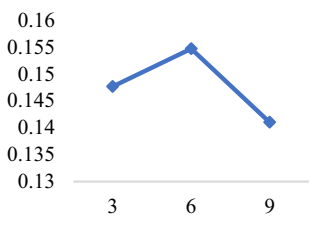
Factor levels [X-Axis]	Pulse on time (µs)	Pulse off time (µs)
Titanium Beta-C alloy	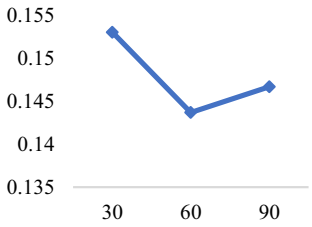	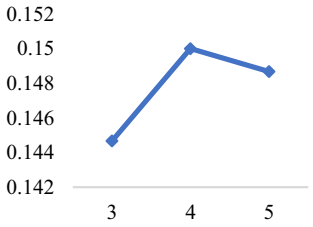
Factor levels [X-Axis]	Voltage (V)	Current (A)

Figure 4: Impact of pulse parameters on the surface roughness.

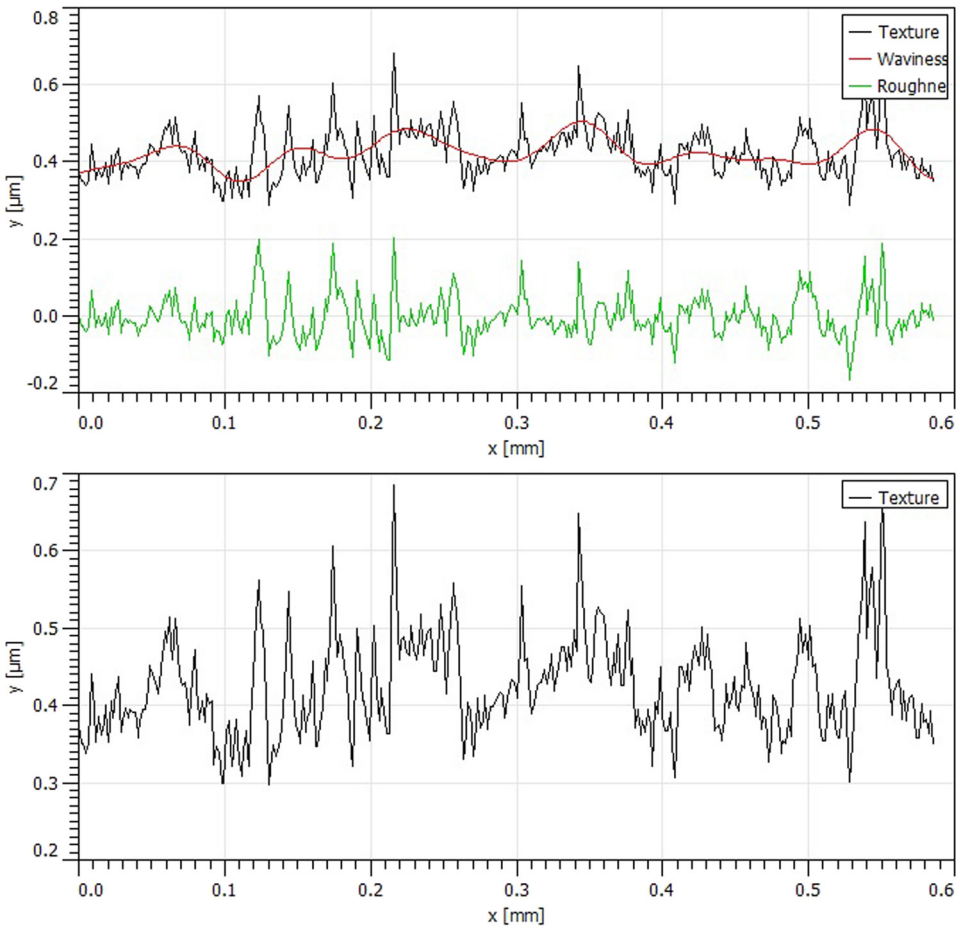

Figure 5: Roughness and waviness outline – best surface finish.

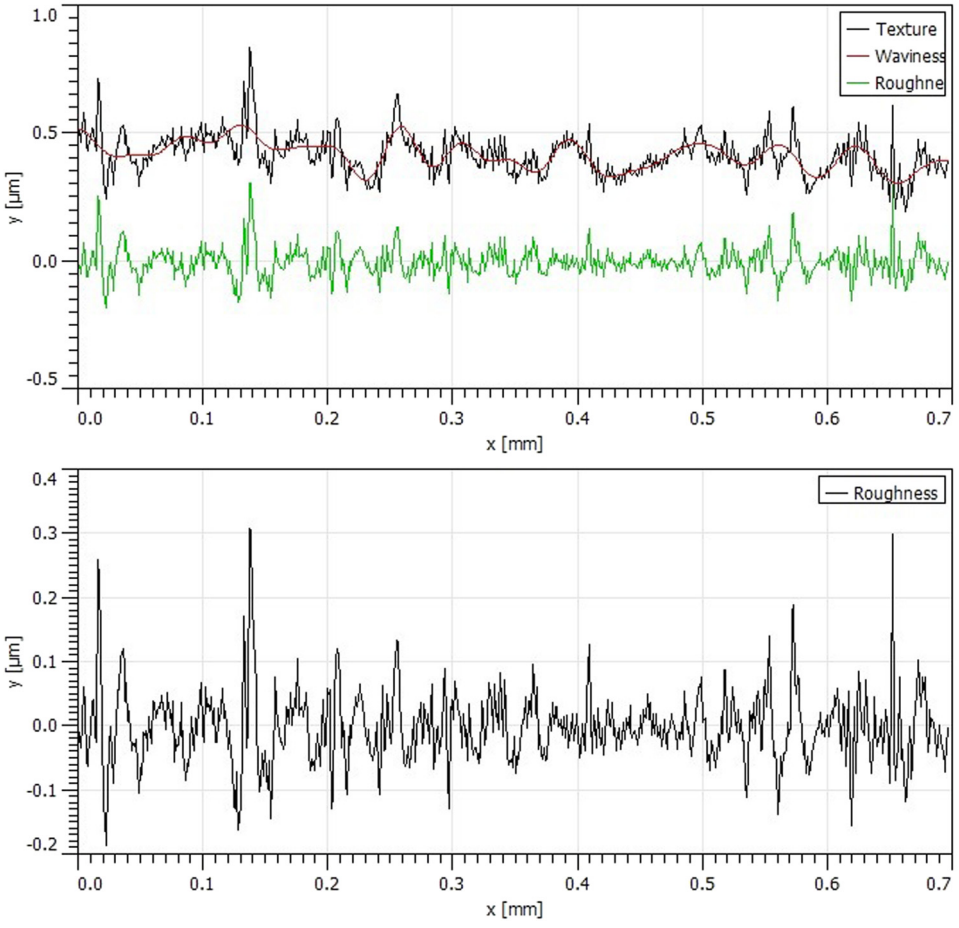

Figure 6: Roughness and waviness outline – worst surface finish.

develop tiny craters arbitrarily on the machined surface that are impacted by the energy of the spark produced. The roughness of this surface is estimated *via* arithmetic average (R_a) [22]. The average surface roughness values obtained in microholes on Titanium Beta-C alloy are presented in Table 6, and the impact of pulse parameters on the surface roughness is shown in Figure 4.

The surface roughness of microholes on Titanium Beta-C alloy increases with increasing pulse on time and current.

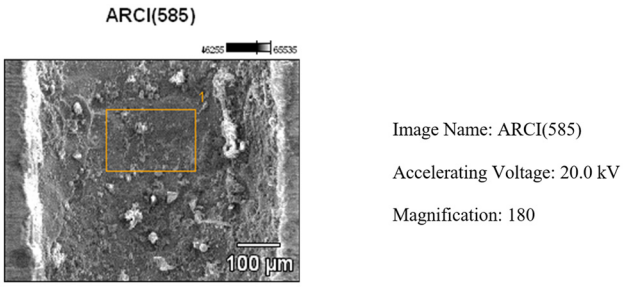

Figure 7: Surface morphology of microhole on Titanium Beta-C alloy.

Surface roughness increases, followed by a decrease with increasing pulse off time. The increased pulse off time provides molten material ample settling time to solidify, due to which there is a chance of increasing surface roughness. An increase in the pulse off time also presents an opportunity to flush the debris *via* the dielectric fluid at high pressure to remove them and reduce the surface roughness. Flushing of the debris by the pressurized dielectric fluid may be responsible for reducing the surface roughness. Surface roughness is seen to decrease initially, followed by a marginal increase with increasing voltage.

A maximum R_a value of 0.172 µm is obtained at a higher pulse on time (9 µs) and higher current (5 A), whereas a least R_a of 0.133 µm is attained for Titanium Beta-C alloy at a low pulse on time (1 µs) and high current (5 A). Irregular texture and craters develop due to the generation of high energy sparks as a result of higher pulse on time and current. Sparking-induced erosion craters have sizes consistent with erosion rates [23].

The surface texture of microhole drilled on Titanium Beta-C alloy in terms of roughness and waviness is

presented in Figure 5 with a least R_a of 0.133 µm. An almost linear pattern is observed for waviness, whereas small peaks and valleys are observed for texture. Similarly, Figure 6 shows the surface texture of microholes drilled on Titanium Beta-C alloy with a peak R_a of 0.172 µm. A bumpy pattern is observed for waviness, whereas high peaks and valleys are observed for texture.

Based on the roughness values and the profile, it can be deduced that a relatively smooth finish is attained in microEDM.

3.2 Surface morphology

The morphology of the microhole surface, entailing basics and form, on Titanium Beta-C alloy, using the microEDM process, is studied using an SEM. Figure 7 displays the surface morphology at upper levels of pulse on time and current. MicroEDM topography exhibits attributes like globules, craters, and voids similar to those seen in the EDM process.

The microdrilled surface on Titanium Beta-C alloy displays uneven surfaces with low depth of crater as a result of quick quenching by the water dielectric, thereby removing the melted material. Second, the microEDM process employs low discharge energy, which leads to a reduction in the crater's breadth and depth. The leftover molten metal experiences rapid solidification, developing overlapping shallow craters that are evenly distributed. SEM imagery divulges evidence of uneven fragments from the erosion process, identifying quick curing of the eroded material by the water dielectric. MicroEDM manifests intense expulsion of the molten metal and related turbulence.

Intense ejection of the molten metal and turbulence linked with it is manifested in this process. MicroEDM employs significantly low discharge energy, thereby generating less molten material accompanied by craters of shrunken breadth and depth. MicroEDM drilled microholes on Titanium Beta-C alloy show the incidence of uneven debris due to erosion. Deionized water is employed as a dielectric fluid. It has high specific heat allowing it to absorb more energy, thereby making it a very good coolant. Swift solidification of the eroded material takes place, thereby forming a consistent chain of overlying shallow craters on the surface. Efficacious elimination of the molten material and debris occurs due to the high cooling effect of deionized water.

3.3 EDXA

It has been reported that the electrode material gets diffused on the workpiece surface in EDM and its variants [24,25]. Hence, EDXA is carried out to investigate this aspect on eroded surfaces of Titanium Beta-C alloy. Figure 8 shows the EDXA spectrum of microEDM-eroded surfaces in Titanium Beta-C alloy. The presence of copper and zinc on the surface signifies dispersion of the electrode material as a result of the use of reverse polarity, *i.e.*, the brass

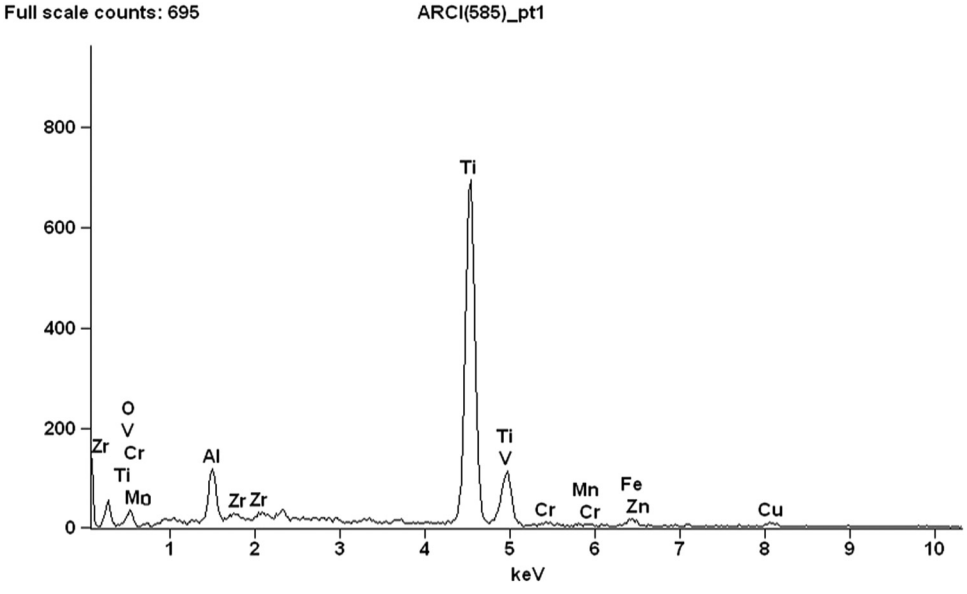

Figure 8: EDXA spectrum.

electrode is positive, and Titanium Beta-C alloy workpiece is negative. The dispersion of the material may occur during ionization. Due to very high temperatures in the interelectrode gap, vaporization and ionization of the electrode material occur. Due to the low ionization potential of the metal atoms, metal atom ionization will be high. As there is a narrow gap between the two electrodes, there is scope for the formation of a bridge for metal transfer. As microEDM and its parent EDM process are spark erosion type, the chances of eroded particles sticking and pushing on opposite surfaces are more.

4 Conclusions

Ensuing conclusions can be synopsized based on the surface integrity studies of microEDM drilled microholes on Titanium Beta-C alloy. In this study, 09 experiments using a brass electrode of 300 μm diameter and resulting in 27 microholes are conducted on Titanium Beta-C alloy. Surface integrity including topographical and morphological studies of spark-eroded surfaces relies on thermal cycles involved in it. In general, microEDM processes utilize relatively lower pulse energies. The use of deionized water as a dielectric impacts the cooling period in a thermal cycle, thereby influencing surface integrity. As a result, cooling rates are higher. A smooth surface finish, as evident from the least R_a value of 0.133 μm obtained at a lower pulse on time of 1 μs and higher current of 5 A, is observed on microEDM surfaces. Roughness is influenced by pulse on time and current variables. Almost a linear pattern is observed for waviness, whereas small peaks and valleys are observed for texture. The microEDM process is characterized by the presence of craters and eroding debris, generally in the form of a residual layer [26]. This investigation has demonstrated the irregular shape of the craters in Titanium Beta-C alloy. This could be attributed to the sudden cooling effect of the melted metal as a result of the water dielectric. Additionally, these surfaces exhibit irregular morphology with shallow crater depths. It is imperative to mention that the microEDM surfaces do not show the presence of cracks. Hence, surface texture and roughness are very important in micromachining. The study carried out will help researchers as well as industries in utilizing the microEDM process for microdrilling of microholes with high-deep holes, *i.e.*, with an aspect ratio of 16.67, on Titanium Beta-C alloy for marine, seawater, oilfield, and other underwater applications.

Acknowledgement: The authors would like to thank VNR-VJIET for providing the necessary resources for carrying out the research work and ARCI Hyderabad for their help in SEM and EDXA.

Funding information: The authors state no funding involved.

Author contributions: Y.S.N.: problem definition, investigation, and data collection. K.J.P.: methodology, original draft writing – review and editing. M.H.R.: experiments, property analysis, and interpretation of results. B.S.B.: literature review, and manuscript review and editing. All authors have accepted responsibility for the entire content of this manuscript and consented to its submission to the journal, reviewed all the results and approved the final version of the manuscript.

Conflict of interest: Authors state no conflict of interest.

References

[1] Mahendran S, Devarajan R, Nagarajan T, Majidi A. A review of micro EDM. Proceedings of the International Multiconference of Engineers and Computer Scientists. 2010. p. 981–6.
[2] Mahendran S, Ramaswamy D. Micro-EDM: Overview and recent developments. National Conference in Mechanical Engineering Research and Postgraduate Students. 2010. p. 480–94.
[3] Masuzawa T, Tanaka K, Nakamura Y, Kinoshita N. Water-based dielectric solution for EDM. CIRP Ann – Manuf Technol. 1985;32(1):119–22. doi: 10.1016/S0007-8506(07)63374-5.
[4] Dhanik S, Joshi SS. Modeling of a single RC-pulse discharge in micro-EDM. Trans ASME, J Manuf Sci Eng. 2005;127(4):759–67. doi: 10.1115/1.2034512.
[5] Jahan MP, Wong YS, Rahman M. A comparative experimental investigation of deep-hole micro-EDM drilling capability for cemented carbide (WC-Co) against austenitic stainless steel (SUS 304). Int J Adv Manuf Technol. 2010;46:1145–60. doi: 10.1007/s00170-009-2167-8.
[6] Noaker PM. EDM's electrifying moves. Manuf Eng. 1996;117:3.
[7] Jesudas T, Arunachalam RM. Study on influence of process parameter in micro - Electrical discharge machining (μ-EDM). Eur J Sci Res. 2011;59(1):115–22.
[8] Rasheed MS, Abidi MH. Analysis of influence of micro-EDM parameters on MRR, TWR and Ra in machining Ni-Ti shape memory alloy. Int J Recent Technol Eng. 2012;1(4):32–7.
[9] Rao GKM, Satyanarayana S, Praveen M. Influence of machining parameters on electric discharge machining of maraging steels - An experimental investigation. World Congress on Engineering 2008. Vol. II. 2008.
[10] Shabgard M, Seyedzavvar M, Oliaei SNB. Influence of input parameters on the characteristics of the EDM process. StrojniskiVestnik/J Mech Eng. 2011;57(9):689–96. doi: 10.5545/sv-jme.2011.035.
[11] Lee HT, Rehbach WP, Tai TY, Hsu FC. Surface integrity in micro-hole drilling using micro-electro discharge machining. Mater Trans. 2003;44(12):2718–22. doi: 10.2320/matertrans.44.2718.
[12] Chaudhary T, Chanda AK, Siddiquee AN, Gangil N. Effect of different dielectric fluids on material removal rate, surface roughness,

kerf width and microhardness. J Braz Soc Mech Sci Eng. 2019;41(344):1–10. doi: 10.1007/s40430-019-1845-1.
[13] Davies OL, En FJvD, Hamaker HC. Design and analysis of industrial experiments. Stat Neerl. 1955;9(4):189–207. doi: 10.1111/j.1467-9574.1955.tb00295.x.
[14] Deepak D, Gowrishankar MC, Shreyas DS. Investigation on the wire electric discharge machining performance of artificially aged Al6061/B4C composites by response surface method. Mater Res. 2022;25:1–11. doi: 10.1590/1980-5373-MR-2022-0010.
[15] Khanna R, Sharma N, Kumar N, Gupta RD, Sharma A. WEDM of Al/SiC/Ti composite: A hybrid approach of RSM-ARAS-TLBO algorithm. Int J Lightweight Mater Manuf. 2022;5(3):315–25. doi: 10.1016/j.ijlmm.2022.04.003.
[16] Paul G, Das M, Ghatak S, Sarkar S, Nagahanumaiah, Mitra S. Investigation on the effect of spark gap in dry μ-electro discharge machining of SiC-10BN nano-composite. Int J Manuf Technol Manag. 2011;24(1–4):71–87. doi: 10.1504/IJMTM.2011.046761.
[17] Pellicer N, Ciurana J, Delgado J. Tool electrode geometry and process parameters influence on different feature geometry and surface quality in electrical discharge machining of AISI H13 steel. J Intell Manuf. 2011;22(4):575–84. doi: 10.1007/s10845-009-0320-8.
[18] Perumal A, Kailasanathan C, Stalin B, Suresh Kumar S, Rajkumar PR, Gangadharan T, et al. Multiresponse optimization of wire electrical discharge machining parameters for Ti-6Al-2Sn-4Zr-2Mo (α - β) alloy using Taguchi-Grey relational approach. Adv Mater Sci Eng. 2022;2022(1):1–13. doi: 10.1155/2022/6905239.
[19] Vaseekaran S, Brown CA. Single discharge, spark erosion in TiB2 and zinc. Part I: Experimental. J Mater Process Technol. 1996;58(1):70–8. doi: 10.1016/0924-0136(95)02109-4.
[20] AZO materials, Titanium alloys – physical properties. Hanson B. The selection and use of titanium: A design guide. Vol. 641, p. 44, Institute of Materials; 1995. https://www.azom.com/article.aspx?ArticleID=1341.
[21] Black JT, Kohser RA, Paul DeGarmo E. DeGarmo's materials and processes in manufacturing. 11th edn. Hoboken, NJ: Wiley; 2012.
[22] Benedict GF. Nontraditional manufacturing processes. 1st edn. Boca Raton: CRC Press; 2017. doi: 10.1201/9780203745410.
[23] Allcock A. New art form for spark erosion. Mach Prod Eng. 1992;150:39–41.
[24] Karmiris-Obratański P, Zagórski K, Papazoglou EL, Markopoulos AP. Surface texture and integrity of electrical discharged machined titanium alloy. Int J Adv Manuf Technol. 2021;115(3):733–47. doi: 10.1007/s00170-020-06159-z.
[25] Thomson PF. Surface damage in electro discharge machining. Mater Sci Technol. 1989;5(11):1153–7. doi: 10.1179/mst.1989.5.11.1153.
[26] Peças P, Henriques E. Influence of silicon powder-mixed dielectric on conventional electrical discharge machining. Int J Mach Tools Manuf. 2003;43(14):1465–71. doi: 10.1016/S0890-6955(03)00169-X.